

SOLUTION TO THE STATIC STABILITY PROBLEM OF THREE-LAYERED ANNULAR PLATES WITH A SOFT CORE

DOROTA PAWLUS

*Faculty of Mechanical Engineering and Computer Science, University of Bielsko-Biala
e-mail: doro@ath.bielsko.pl*

The solutions to the static stability problem of a three-layered annular plate with a soft core and a symmetric cross-section structure are presented in this paper. The basic element of the solution is the formulation of a system of differential equations describing plate deflections and the use of the finite difference method in calculation of critical loads of buckling forms solving the eigen-value problem. The solution indicates the minimal values of static critical loads as well as the buckling forms of plates compressed on a selected edge. The obtained results have been compared with those obtained for plate models built by means of the finite element method. The final remarks concerning the forms of the loss of static stability of analysed plates with the sandwich structure have been formulated. This paper is a complement of the work by Pawlus (2005), which concerned calculations of the dynamic stability of plates, and it is an extension to cases of wave forms of the plate buckling problem earlier presented only for regular, axially-symmetrical forms of deformation in, eg., Pawlus (2002).

Key words: sandwich, annular plate; static stability; buckling form; finite differences method; FEM

1. Introduction

The evaluation of critical static loads with the indication of the minimal value and the corresponding form of plate buckling is the basic problem in plate stability analysis. The analysis of static critical loads precedes the evaluation of dynamic critical loads of plates and the observation of their supercritical behaviour.

Buckling loads and geometrically nonlinear axisymmetric postbuckling behaviour of cylindrically orthotropic annular plates under inplane radial compressive load applied to the outer edge were undertaken by Dumir and Shingal

(1985). Geometrically nonlinear, axisymmetric, moderately large deflections of laminated annular plates were presented by Dumir *et al.* (2001). Also in the work by Krizhevsky and Stavsky (1996) laminated annular plates were examined. Buckling loads of such plates uniformly compressed in the radial direction were analysed, too. The axisymmetric dynamic stability of sandwich circular plates with viscoelastic damping layer under periodic radial loading along the outer edge was the subject of considerations by Wang and Chen (2003). Also the axisymmetric dynamic instability of a rotating sandwich annular plate with a viscoelastic core under periodic radial stress was examined by Chen *et al.* (2006).

Solutions to the static analysis of plate stability presented in this paper refer to the solutions of the three-layer annular plate problem presented by Pawlus (2005). They exactly constitute the introduction to the dynamic stability plate problem undertaken in the mentioned work. The presented solutions do not limit the range of the examined plates only to such forms of deformations which are regular and axially-symmetrical (see Pawlus, 2002), but they are global solutions for different circumferential wave forms of the loss of plate static stability. The presented solutions eliminate possible questions connected with forms of the plate buckling for minimal values of critical loads. They also show that the variability in number of waves of deformation plates strongly depends on geometric and material properties of layers in plate structures. Two solutions presented in this paper use approximation methods: finite differences and finite elements. The proposed solution to the static stability of analysed three-layer annular plate, which uses the finite difference method, refers to solutions of homogeneous elastic plates presented, eg. by Wojciech (1979) as well as by Trombski and Wojciech (1981). Additionally, some modification of calculation algorithms to formulas necessary for sandwich structures is introduced.

2. Problem formulation

A three-layer annular plate with a symmetric cross-section structure composed of thin steel facings and a soft foam isotropic core is considered. Plate edges are clamped. Compressive loads uniformly distributed on the plate perimeter act on the outer or/and inner edge of the plate facings. A scheme of the plate is presented in Fig. 1.

In the solution based on the finite difference method, the classical theory of sandwich plates with the broken line hypothesis (Volmir, 1967) is adopted. The

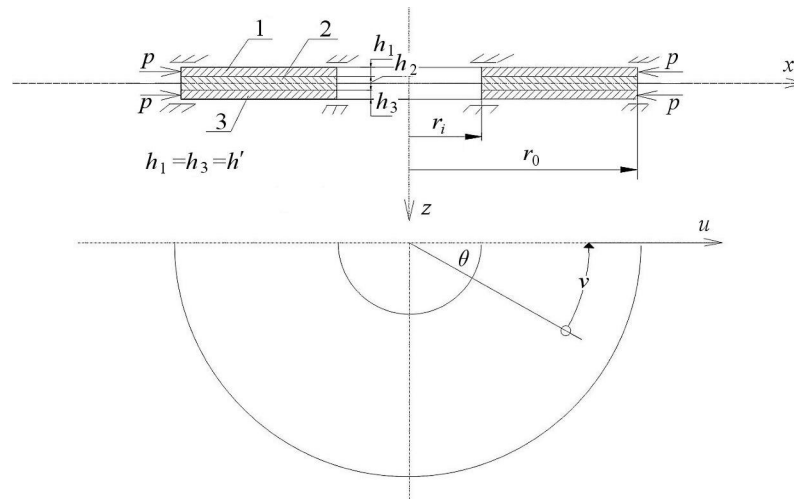


Fig. 1. Scheme of analysed plate

classical participation of plate layers in carrying the plate load is assumed: the facings are loaded with normal but the core with shear stresses. Equal values of transverse deflections of plate layers are accepted. The minimal critical static load of the plate and the corresponding form of buckling are calculated analysing the minimal critical loadings found from the eigen-value problem for different numbers m of plate circumferential waves describing the form of plate deformation.

3. System of elementary equations

In the group of presented basic equations – the obtained equation, (3.14), enabling calculation of transverse plate deflections is fundamental. The quantities describing the relative radial δ and circumferential displacements γ of plate facings coming from the sandwich structure of the analysed plate build additional expressions in equation (3.14) in relation to the formulas of homogeneous plates.

3.1. Equilibrium equations

The system of forces acting on each of three layers of a single annular sector of the plate is presented in Fig. 2. The system of equilibrium equations of each layer is presented by the formulas:

— layer 1

$$\begin{aligned}
 & \frac{M_{r_1} - M_{\theta_1}}{r} + M_{r_1'r} + \frac{1}{r}M_{\theta r_1'\theta} - Q_{r_1} + \frac{h_1}{2}\tau_{r_1} = 0 \\
 & \frac{1}{r}M_{\theta_1'\theta} + \frac{2}{r}M_{r\theta_1} + M_{r\theta_1'r} - Q_{\theta_1} + \frac{h_1}{2}\tau_{\theta_1} = 0 \\
 & (T_{\theta r_1}w_r)'_{\theta} + (T_{\theta r_1}w_{\theta})'_{r} + (rN_{r_1}w_r)'_{r} + \frac{1}{r}(N_{\theta_1}w_{\theta})'_{\theta} + \\
 & \quad + Q_{\theta_1'\theta} + (rQ_{r_1})'_{r} + r\tau_{r_1}w_r + \tau_{\theta_1}w_{\theta} = 0
 \end{aligned} \tag{3.1}$$

— layer 2

$$\begin{aligned}
 -Q_{r_2} + \frac{h_2}{2}\tau_{r_1} + \frac{h_2}{2}\tau_{r_3} = 0 & \quad -Q_{\theta_2} + \frac{h_2}{2}\tau_{\theta_1} + \frac{h_2}{2}\tau_{\theta_3} = 0 \\
 Q_{\theta_2'\theta} + (rQ_{r_2})'_{r} - r\tau_{r_1}w_r + r\tau_{r_3}w_r - \tau_{\theta_1}w_{\theta} + \tau_{\theta_3}w_{\theta} = 0
 \end{aligned} \tag{3.2}$$

— layer 3

$$\begin{aligned}
 & \frac{M_{r_3} - M_{\theta_3}}{r} + M_{r_3'r} + \frac{1}{r}M_{\theta r_3'\theta} - Q_{r_3} + \frac{h_3}{2}\tau_{r_3} = 0 \\
 & \frac{1}{r}M_{\theta_3'\theta} + \frac{2}{r}M_{r\theta_3} + M_{r\theta_3'r} - Q_{\theta_3} + \frac{h_3}{2}\tau_{\theta_3} = 0 \\
 & (T_{\theta r_3}w_r)'_{\theta} + (T_{\theta r_3}w_{\theta})'_{r} + (rN_{r_3}w_r)'_{r} + \frac{1}{r}(N_{\theta_3}w_{\theta})'_{\theta} + \\
 & \quad + Q_{\theta_3'\theta} + (rQ_{r_3})'_{r} - r\tau_{r_3}w_r - \tau_{\theta_3}w_{\theta} = 0
 \end{aligned} \tag{3.3}$$

where

- $N_{r_1(3)}, N_{\theta_1(3)}$ — normal radial and circumferential forces acting on facings per unit length, respectively
- $Q_{r_1(2,3)}, Q_{\theta_1(2,3)}$ — transverse forces acting on facings and core layer per unit length, respectively
- $M_{r_1(3)}, M_{\theta_1(3)}$ — elementary radial and circumferential bending moments of facings, respectively
- $M_{r\theta_1(3)}$ — elementary torsional moments of outer layers
- $T_{\theta r_1(3)}$ — shear forces per unit length acting on outer plate layers
- $\tau_{r_1(3)}, \tau_{\theta_1(3)}$ — shearing radial and circumferential stresses, respectively
- w — plate deflection.

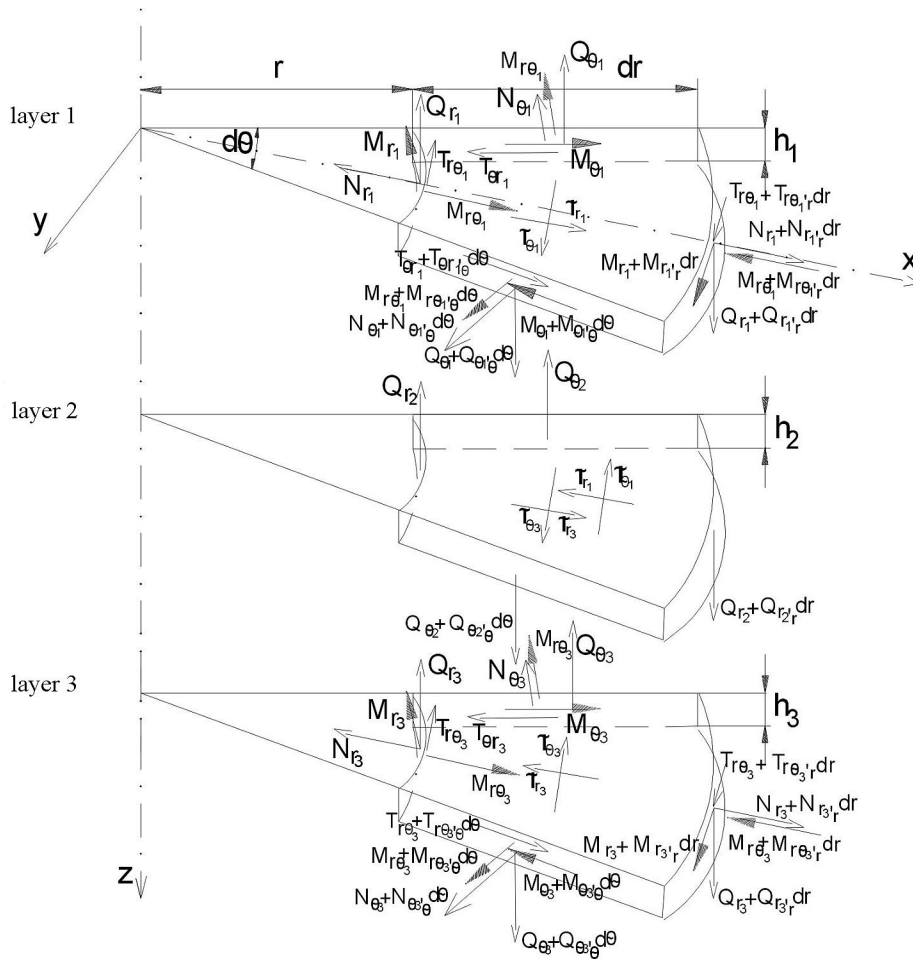


Fig. 2. Loading of plate layers

3.2. Geometric relations

Radial and circumferential cross-section deformations of the plate structure are shown in Fig. 3. The angles β and α determine the radial and circumferential deformation of the plate core, respectively. They are expressed by equations

$$\beta = \frac{u_1 - u_3 - w_r h'}{h_2} \quad \alpha = \frac{v_1 - v_3 - \frac{1}{r} w_\theta h'}{h_2} \quad (3.4)$$

where

- $u_{1(3)}, v_{1(3)}$ – displacements of the points of the middle plane of facings in the radial and circumferential directions, respectively
- $h' = h_1 = h_3$ – thicknesses of the plate layers.

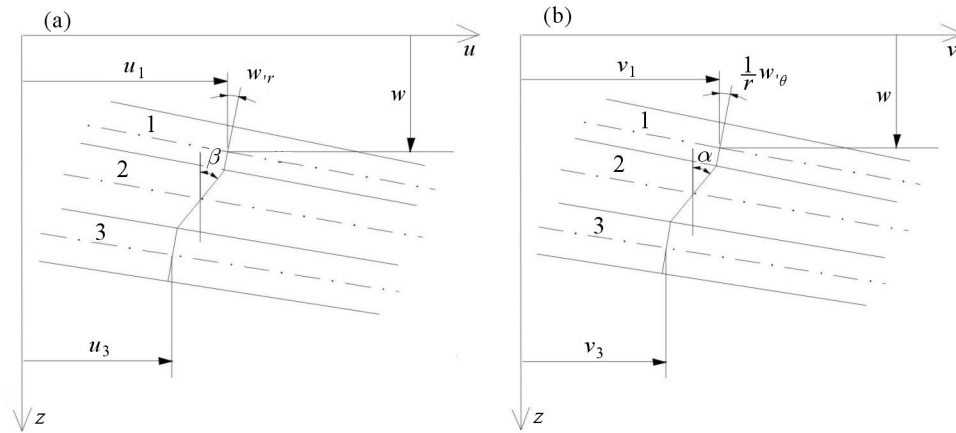


Fig. 3. Cross-sectional geometry of sandwich plate: (a) in radial direction, (b) in circumferential direction

3.3. Physical relations

Linear physical relations of Hooke's law for the plane stress state in plate outer layers are given by the following formulas

$$\sigma_{r_i} = \frac{E_i}{1 - \nu_i^2} (\varepsilon_{r_i} + \nu \varepsilon_{\theta_i}) \quad \sigma_{\theta_i} = \frac{E_i}{1 - \nu_i^2} (\varepsilon_{\theta_i} + \nu \varepsilon_{r_i}) \quad (3.5)$$

where i denotes the outer layer, $i = 1$ or 3 .

Young's moduli and Poisson's ratios of the facing material fulfil the conditions: $E = E_1 = E_3$ and $\nu = \nu_1 = \nu_3$.

The physical relations of the core material under shearing stress are as follows

$$\tau_{rz_2} = G_2 \gamma_{rz_2} \quad \tau_{\theta z_2} = G_2 \gamma_{\theta z_2} \quad (3.6)$$

where $\gamma_{rz_2}, \gamma_{\theta z_2}$ – shearing strain of the core in the radial and circumferential directions, respectively

$$\gamma_{rz_2} = u_{2,z}^{(z)} + w_{,r} \quad \gamma_{\theta z_2} = v_{2,z}^{(z)} + \frac{1}{r} w'_{,\theta}$$

and $u_2^{(z)} = u_2 - z\beta$, $v_2^{(z)} = v_2 - z\alpha$ – radial and circumferential displacements of a point with the z – coordinate, respectively (z is the distance between the point and the middle surface of the core).

3.4. Differential equations for plate deflections

Based on the relations between sectional forces, moments and stresses for plate facings, equations of sectional forces and moments have been established

$$\begin{aligned}
 N_{r_i} &= \frac{Eh_i}{1-\nu^2} \left(u_{i'r} + \frac{\nu}{r}u_i + \frac{\nu}{r}v_{i\theta} + \frac{1}{2}(w'_{r'})^2 + \frac{\nu}{2r^2}(w'_{\theta})^2 \right) \\
 N_{\theta_i} &= \frac{Eh_i}{1-\nu^2} \left(\frac{1}{r}u_i + \frac{1}{r}v_{i\theta} + \nu u_{i'r} + \frac{\nu}{2}(w'_{r'})^2 + \frac{1}{2r^2}(w'_{\theta})^2 \right) \\
 T_{r\theta_i} &= Gh_i \left(\frac{1}{r}u_{i\theta} + v_{i'r} - \frac{1}{r}v_i + \frac{1}{r}w'_{r'}w'_{\theta} \right) \\
 M_{r_i} &= -D_i \left(w'_{rr} + \frac{\nu}{r}w'_{r'} + \frac{\nu}{r^2}w'_{\theta\theta} \right) \\
 M_{\theta_i} &= -D_i \left(\frac{1}{r^2}w'_{\theta\theta} + \frac{1}{r}w'_{r'} + \nu w'_{rr} \right) \\
 M_{r\theta_i} &= -2D_{r\theta_i} \left(\frac{w}{r} \right)'_{r\theta}
 \end{aligned} \tag{3.7}$$

where D_i , $D_{r\theta_i}$ denote the flexural rigidities of the outer layers, and

$$D_i = \frac{Eh_i^3}{12(1-\nu^2)} \quad D_{r\theta_i} = \frac{Gh_i^3}{12}$$

The transverse forces Q_{r_2} and Q_{θ_2} respectively expressed by formulas $Q_{r_2} = \tau_{rz_2}h_2$, $Q_{\theta_2} = \tau_{\theta z_2}h_2$, have been obtained using equations (3.4) and (3.6)

$$Q_{r_2} = G_2(\delta + H'w'_{r'}) \quad Q_{\theta_2} = G_2 \left(\gamma + H' \frac{1}{r}w'_{\theta} \right) \tag{3.8}$$

where

$$\delta = u_3 - u_1 \quad \gamma = v_3 - v_1 \quad H' = h' + h_2 \tag{3.9}$$

Finding from equations (3.1)_{1,2}, (3.2)_{1,2} and (3.3)_{1,2} formulas determining the radial $Q_{r1(2,3)}$ and circumferential $Q_{\theta1(2,3)}$ forces, enables one to obtain the resultant forces Q_r and Q_θ as the sums of the individual layer forces

$$\begin{aligned}
Q_r &= \frac{1}{r}(M_{r_1} + M_{r_3}) - \frac{1}{r}(M_{\theta_1} + M_{\theta_3}) + (M_{r_1} + M_{r_3})'_r + \\
&\quad + \frac{1}{r}(M_{\theta r_1} + M_{\theta r_3})'_\theta + \frac{H'}{h_2}Q_{r_2}
\end{aligned} \tag{3.10}$$

$$Q_\theta = \frac{1}{r}(M_{\theta_1} + M_{\theta_3})'_\theta + (M_{r\theta_1} + M_{r\theta_3})'_r + \frac{2}{r}(M_{\theta r_1} + M_{\theta r_3}) + \frac{H'}{h_2}Q_{\theta_2}$$

Inserting equations (3.7)₄₋₆ and (3.8) into equations (3.10) yields the following formulas

$$\begin{aligned}
Q_r &= -k_1 w'_{rrr} - \frac{k_1}{r} w'_{rr} + \frac{k_1}{r^2} w'_r - \frac{k_2}{r^2} w'_{r\theta\theta} + \frac{k_1 + k_2}{r^3} w_{\theta\theta} + \\
&\quad + G_2(\delta + H' w'_r) \frac{H'}{h_2}
\end{aligned} \tag{3.11}$$

$$Q_\theta = -\frac{k_1}{r^3} w_{\theta\theta\theta} - \frac{k_1}{r^2} w'_{\theta r} - \frac{k_2}{r} w'_{\theta rr} + G_2\left(\gamma + H' \frac{1}{r} w_{\theta}\right) \frac{H'}{h_2}$$

where $k_1 = 2D$, $k_2 = 4D_{r\theta} + \nu k_1$.

Adding the summands of equations (3.1)₃, (3.2)₃, (3.3)₃ all together gives the following equation

$$(T_{r\theta} w'_r)'_\theta + (T_{\theta r} w'_\theta)'_r + (r N_r w'_r)'_r + \frac{1}{r} (N_\theta w'_\theta)'_\theta + Q_{\theta_\theta} + (r Q_r)'_r = 0 \tag{3.12}$$

In the above equation, (3.12) the resultant membrane forces N_r , N_θ , $T_{r\theta}$ are expressed respectively: $N_r = N_{r_1} + N_{r_3}$, $N_\theta = N_{\theta_1} + N_{\theta_3}$ and $T_{r\theta} = T_{r\theta_1} + T_{r\theta_3}$. They have been determined by means of the introduced stress function Φ

$$\begin{aligned}
N_r &= 2h' \left(\frac{1}{r} \Phi'_{r'} + \frac{1}{r^2} \Phi'_{\theta\theta} \right) & N_\theta &= 2h' \Phi'_{rr} \\
T_{r\theta} &= 2h' \left(\frac{1}{r^2} \Phi'_{\theta} - \frac{1}{r} \Phi'_{r\theta} \right)
\end{aligned} \tag{3.13}$$

Inserting (3.11) and (3.13) into equation (3.12) yields a differential equation for deflections of the analysed plate

$$\begin{aligned}
& k_1 w'_{rrrr} + \frac{2k_1}{r} w'_{rrr} - \frac{k_1}{r^2} w'_{rr} + \frac{k_1}{r^3} w'_r + \frac{k_1}{r^4} w'_{\theta\theta\theta\theta} + \frac{2(k_1 + k_2)}{r^4} w'_{\theta\theta} + \frac{2k_2}{r^2} w'_{rr\theta\theta} + \\
& - \frac{2k_2}{r^3} w'_{r\theta\theta} - G_2 \frac{H'}{h_2} \frac{1}{r} \left(\gamma'_{\theta} + \delta + r\delta'_r + H' \frac{1}{r} w'_{\theta\theta} + H' w'_r + H' r w'_{rr} \right) = \\
& = \frac{2h'}{r} \left(\frac{2}{r^2} \Phi'_{\theta} w'_{r\theta} - \frac{2}{r} \Phi'_{\theta r} w'_{\theta r} + \frac{2}{r^2} w'_{\theta} \Phi'_{\theta r} - \frac{2}{r^3} \Phi'_{\theta} w'_{\theta} + w'_{\theta} \Phi'_{rr} + \Phi'_{\theta r} w'_{rr} + \right. \\
& \left. + \frac{1}{r} \Phi'_{\theta\theta} w'_{rr} + \frac{1}{r} \Phi'_{rr} w'_{\theta\theta} \right)
\end{aligned} \tag{3.14}$$

3.5. Boundary conditions

The boundary conditions for the loading are expressed by equations

$$\sigma_r \Big|_{r=r_i} = -pd_1 \qquad \sigma_r \Big|_{r=r_0} = -pd_2 \tag{3.15}$$

where d_1, d_2 are some quantities being 0 or 1, which determine the loading of the inner or/and the outer plate edge (Wojciech, 1978). The boundary conditions for the clamped edges of the plate are as follows

$$\begin{aligned}
w \Big|_{r=r_0(r_i)} &= 0 & w'_r \Big|_{r=r_0(r_i)} &= 0 & \delta \Big|_{r=r_0(r_i)} &= 0 \\
\delta'_r \Big|_{r=r_0(r_i)} &= 0 & \gamma \Big|_{r=r_0(r_i)} &= 0 & \gamma'_r \Big|_{r=r_0(r_i)} &= 0
\end{aligned} \tag{3.16}$$

4. Problem solution

The quantities δ and γ , unknown in equations (3.14), have been obtained by finding the differences in the radial and circumferential displacements u_1, u_3 and v_1, v_3 of points from the middle surface of the plate facings (3.9) using the equilibrium equations for forces acting on the undeformed outer plate layers in the u and v direction, respectively:

— layer 1

$$N_{r_1} + rN_{r_1'r} - N_{\theta_1} + T_{\theta r_1'\theta} + r\tau_{r_1} = 0 \tag{4.1}$$

$$N_{\theta_1'\theta} + 2T_{r\theta_1} + rT_{r\theta_1'r} + r\tau_{\theta_1} = 0$$

— layer 3

$$N_{r_3} + rN_{r_3'r} - N_{\theta_3} + T_{\theta r_3'\theta} - r\tau_{r_3} = 0 \tag{4.2}$$

$$N_{\theta_3'\theta} + 2T_{r\theta_3} + rT_{r\theta_3'r} - r\tau_{\theta_3} = 0$$

Having calculated the above expressions, the summands in equations (4.1) and (4.2) have been subtracted and then expressions (3.7)₁₋₃, which determine the sectional forces N_{r_i} , N_{θ_i} , $T_{r\theta_i}$, have been inserted into the obtained equations. The shearing stresses τ_r , τ_θ have been expressed by sums of stresses τ_{r_1} , τ_{r_3} and τ_{θ_1} , τ_{θ_3} using equations (3.2)_{1,2}

$$\tau_{r_1} + \tau_{r_3} = \frac{2}{h_2} Q_{r_2} \quad \tau_{\theta_1} + \tau_{\theta_3} = \frac{2}{h_2} Q_{\theta_2}$$

After some transformations, the following differential equations have been found

$$\begin{aligned} \frac{2r}{h_2} G_2 H' w_{,r} &= \frac{Eh'}{1-\nu^2} \left(r\delta_{,rr} + \delta_{,r} - \frac{1}{r}\delta + \nu\gamma'_{r\theta} - \frac{1}{r}\gamma'_{\theta} \right) + \\ &+ Gh' \frac{1}{r} (\delta'_{\theta\theta} + r\gamma'_{r\theta} - \gamma'_{\theta}) - \frac{2r}{h_2} G_2 \delta \\ \frac{2}{h_2} G_2 H' w_{,\theta} &= \frac{Eh'}{1-\nu^2} \left(\frac{1}{r}\delta'_{\theta} + \nu\delta'_{r\theta} + \frac{1}{r}\gamma'_{\theta\theta} \right) - \frac{2r}{h_2} G_2 \gamma + \\ &+ Gh' \frac{1}{r} (\delta'_{\theta} + r\delta'_{r\theta} + r^2\gamma'_{rr} + r\gamma'_{r} - \gamma) \end{aligned} \quad (4.3)$$

Using the following dimensionless quantities and the expressions in the solution

$$\begin{aligned} F &= \frac{\Phi}{Eh^2} & \zeta &= \frac{w}{h} & \rho &= \frac{r}{r_0} \\ \bar{\delta} &= \frac{\delta}{h} & \zeta(\rho, \theta) &= X(\rho) \cos(m\theta) & \bar{\gamma} &= \frac{\gamma}{h} \\ \bar{\delta}(\rho, \theta) &= \bar{\delta}(\rho) \cos(m\theta) & \bar{\gamma}(\rho, \theta) &= \bar{\gamma}(\rho) \sin(m\theta) \end{aligned} \quad (4.4)$$

where m is the number of circumferential waves corresponding to the form of plate buckling, $h = h_1 + h_2 + h_3$ - total thickness of plate, equations (3.14) and (4.3) can be presented in the following form

$$\begin{aligned} W_1 X'_{,\rho\rho\rho\rho} + \frac{2W_1}{\rho} X'_{,\rho\rho\rho} - \frac{W_3}{\rho^2} X'_{,\rho\rho} + \frac{W_3}{\rho^3} X'_{,\rho} + \frac{W_4}{\rho^4} X - \frac{2W_1}{\rho^4} m^2 X + \\ - \frac{W_5}{\rho} H' \left(m\bar{\gamma} + \bar{\delta} + \rho\bar{\rho}'_{,\rho} - \frac{m^2}{\rho} \frac{H'}{r_0} X + \frac{H'}{r_0} X'_{,\rho} + \frac{H}{r_0} \rho X'_{,\rho\rho} \right) = \\ = \frac{2W_5^2 W_2}{\rho} \left(X'_{,\rho} Y_{0\rho} + Y_0 X'_{,\rho\rho} - \frac{m^2}{\rho} X Y_{0\rho} \right) \\ X'_{,\rho} = \bar{\delta} \left(A \frac{1}{\rho^2} + B + \frac{m^2}{\rho^2} C \right) - A \frac{1}{\rho} \bar{\delta}'_{,\rho} - A \bar{\delta}'_{,\rho\rho} - m \frac{K_2}{\rho} \bar{\gamma}'_{,\rho} + m \frac{K_1}{\rho^2} \bar{\gamma} \\ mX = -m \frac{K_1}{\rho} \bar{\delta} - mK_2 \bar{\delta}'_{,\rho} + \rho C \bar{\gamma}'_{,\rho\rho} + C \bar{\gamma}'_{,\rho} - \bar{\gamma} \left(m^2 \frac{A}{\rho} + \frac{C}{\rho} + B\rho \right) \end{aligned} \quad (4.5)$$

where

$$\begin{aligned}
 Y_0 &= F'_{,\rho} & A &= -\frac{Eh'}{1-\nu^2} \frac{h_2}{G_2} \frac{1}{2H'r_0} & B &= -\frac{r_0}{H'} \\
 C &= -\frac{Gh'}{r_0} \frac{h_2}{2G_2H'} & D &= A\nu & K_1 &= A + C \\
 K_2 &= D + C & W_1 &= k_1 \frac{h'}{h} \frac{h_2}{G_2} \frac{1}{r_0^3} & W_2 &= E \frac{h_2}{G_2} \frac{h^3}{r_0^3} \\
 W_{12} &= k_2 \frac{h'}{h} \frac{h_2}{G_2} \frac{1}{r_0^3} & W_3 &= W_1 + 2m^2W_{12} & W_5 &= \frac{h'}{h} \\
 W_4 &= m^4W_1 - 2m^2W_{12}
 \end{aligned}$$

Assuming that the stress function F is a solution to the disk state and using the boundary conditions for the clamped edges, based on the work by Wojciech (1978), the following expression has been obtained

$$Y_0 = K_{10}p^* \left(e_1\rho + \frac{e_2}{\rho} \right) \quad (4.6)$$

where

$$K_{10} = \frac{r_0^2}{h^2} \quad p^* = \frac{p}{E} \quad e_1 = \frac{\frac{d_2}{\rho_i} - d_1\rho_i}{\rho_i - \frac{1}{\rho_i}} \quad e_2 = \frac{d_1\rho_i - \rho_i d_2}{\rho_i - \frac{1}{\rho_i}}$$

and ρ_i is the dimensionless inner plate radius.

In the solution, the finite difference method has been used for the approximation of the derivatives with respect to ρ by central differences in discrete points. Transformed equations (4.5) have the forms

$$\begin{aligned}
 \mathbf{M}_{AP}\mathbf{U} + \mathbf{M}_{AD}\mathbf{D} + \mathbf{M}_{AG}\mathbf{G} &= p^*\mathbf{M}_{AC}\mathbf{U} \\
 \mathbf{M}_{ACP}\mathbf{U} &= \mathbf{M}_{ACD}\mathbf{D} + \mathbf{M}_{ACG}\mathbf{G} & \mathbf{M}_P\mathbf{U} &= \mathbf{M}_D\mathbf{D} + \mathbf{M}_G\mathbf{G}
 \end{aligned} \quad (4.7)$$

where:

\mathbf{U} , \mathbf{D} , \mathbf{G} – vectors of plate deflections and differences of the radial u_i and circumferential v_i displacements of facings (3.9), respectively

\mathbf{M}_{AP} , \mathbf{M}_{AC} , \mathbf{M}_{ACD} , \mathbf{M}_{ACG} , \mathbf{M}_D , \mathbf{M}_G – matrices of elements composed of geometric and material parameters of the plate and the quantity b of the length of the interval in the finite difference method and the number m of buckling waves

\mathbf{M}_{AD} – matrix of geometric parameters and the quantity b

\mathbf{M}_{AG} – matrix of geometric parameters and the number m

\mathbf{M}_{ACP} – matrix with elements described by the quantity $1/(2b)$

\mathbf{M}_P – matrix with elements described by the number m .

Solving the eigen-value problem, the minimal value of p^* as the critical static load p_{cr}^* has been calculated

$$\det[(\mathbf{M}_{AP} + \mathbf{M}_{AD}\mathbf{M}_{ATD} + \mathbf{M}_{AG}\mathbf{M}_{ATG}) - p^*\mathbf{M}_{AC}] = 0 \quad (4.8)$$

and \mathbf{M}_{ATG} , \mathbf{M}_{ATD} are matrices obtained from transformed equations (4.7)_{2,3} in the forms

$$\mathbf{M}_{ATG} = \mathbf{M}_{TG}^{-1}(\mathbf{M}_P - \mathbf{M}_D\mathbf{M}_{ACD}^{-1}\mathbf{M}_{ACP}) \quad (4.9)$$

$$\mathbf{M}_{ATD} = \mathbf{M}_{ACD}^{-1}\mathbf{M}_{ACP} - \mathbf{M}_{ACD}^{-1}\mathbf{M}_{ACG}\mathbf{M}_{ATG}$$

where

$$\mathbf{M}_{TG} = \mathbf{M}_G - \mathbf{M}_D\mathbf{M}_{ACD}^{-1}\mathbf{M}_{ACG}$$

5. Numerical calculations

Exemplary numerical calculations of a plate loaded on the inner or/and outer edges have been carried out by analysing the influence of geometric and material parameters on the critical static loads and corresponding forms of buckling.

The calculations have been carried out for plates with the following geometrical dimensions: inner radius $r_i = 0.2$ m, outer radius $r_0 = 0.5$ m, various core and steel facing thicknesses in the range of: $h_2 = 0.005$ m, 0.01 m, 0.02 m and $h' = 0.0005$ m, 0.001 m, respectively; accepting a polyurethane foam as an isotropic core material with Kirchhoff's moduli $G_2 = 5$ MPa (Majewski and Maćkowski, 1975) and $G_2 = 15.82$ MPa (Romanów, 1995) and the Poisson's ratio $\nu = 0.3$ (PN-84/B-03230).

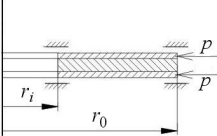
5.1. Calculations by finite difference method

Calculations of plates using the Finite Difference Method (FDM) have been preceded by analysis of the accuracy of values of the critical loads for different numbers N of discrete points: $N = 11, 14, 17, 21, 26$. Tables 1, 2, 3, 4 show the critical plate loads p_{cr} for different buckling forms determined

by the number m of circumferential waves. The minimal critical load with the wave number m have been marked. The analysis of critical loads p_{cr} indicates that the number $N = 14$ of discrete points fulfils the accuracy up to 5% of technical error. The calculations were carried out for this number ($N = 14$) of discrete points in FDM. The results show that for a higher number N of discrete points, $N = 21, 26$, the form of plate buckling has an additional circumferential wave for the minimal critical plate load p_{cr} .

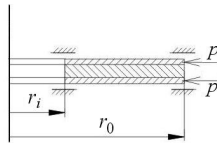
The influence of core Kirchhoff's modulus and layer thicknesses, particularly the core on the distribution of critical loads and the forms of plate buckling are presented in Fig. 4- Fig. 6.

Table 1. Critical plate loads p_{cr} for different wave numbers m

	$d_1 = 0$	$d_2 = 1$	$E = 2.1 \cdot 10^5 \text{ MPa}$
	$r_i = 0.2 \text{ m}$	$r_0 = 0.5 \text{ m}$	$h' = 0.001 \text{ m}$
	$\nu = 0.3$	$G_2 = 5 \text{ MPa}$	$h_2 = 0.005 \text{ m}$

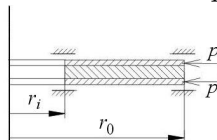
m	$p_{cr} \text{ [MPa]}$				
	N				
	11	14	17	21	26
0	32.78	32.89	32.94	32.98	33.01
1	30.95	31.06	31.12	31.16	31.19
2	26.89	27.01	27.09	27.14	27.18
3	23.32	23.45	23.53	23.59	23.63
4	21.25	21.37	21.44	21.50	21.54
5	20.41	20.52	20.58	20.63	20.67
6	20.44	20.53	20.58	20.62	20.65
7	21.05	21.13	21.17	21.21	21.24
8	22.09	22.16	22.22	22.24	22.26

All analysed examples of plates loaded on the inner perimeter of facings confirmed the observation earlier noticed in homogeneous plates (Wojciech, 1978; Pawlus, 1996) that the buckling of plates with double clamped edges for the minimal critical static load has a regular, axi-symmetrical form. Figure 4 shows a suitable distribution of the critical loads. Detailed results for such loaded plates, including their behaviour, were presented by Pawlus (2002, 2003). Diagrams 5, 6 present the distribution of critical loads for the plate compressed at outer perimeters depending on the number m of buckling waves. The points marked by * in the diagrams correspond to forms of buckling of plates loaded with minimal critical loads. The presented results indicate a change in

Table 2. Critical plate loads p_{cr} for different wave numbers m


$d_1 = 0$	$d_2 = 1$	$E = 2.1 \cdot 10^5 \text{ MPa}$
$r_i = 0.2 \text{ m}$	$r_0 = 0.5 \text{ m}$	$h' = 0.0005 \text{ m}$
$\nu = 0.3$	$G_2 = 5 \text{ MPa}$	$h_2 = 0.02 \text{ m}$

$p_{cr} \text{ [MPa]}$					
m	N				
	11	14	17	21	26
0	118.77	118.95	119.04	119.11	119.16
9	70.31	70.44	70.54	70.64	70.72
10	69.70	69.83	69.92	70.01	70.09
11	69.41	69.53	69.62	69.71	69.79
12	69.38	69.49	69.58	69.67	69.74
13	69.55	69.67	69.75	69.83	69.90
14	69.91	70.02	70.10	70.18	70.25

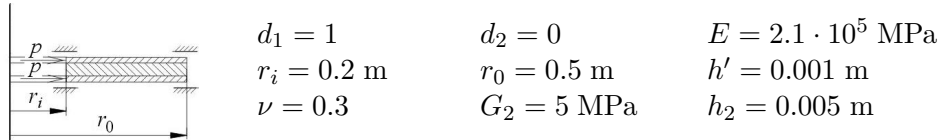
Table 3. Critical plate loads p_{cr} for different wave numbers m


$d_1 = 0$	$d_2 = 1$	$E = 2.1 \cdot 10^5 \text{ MPa}$
$r_i = 0.2 \text{ m}$	$r_0 = 0.5 \text{ m}$	$h' = 0.001 \text{ m}$
$\nu = 0.3$	$G_2 = 15.82 \text{ MPa}$	$h_2 = 0.005 \text{ m}$

$p_{cr} \text{ [MPa]}$					
m	N				
	11	14	17	21	26
0	76.10	76.19	76.23	76.27	76.30
3	54.84	55.08	55.22	55.33	55.42
4	49.81	50.04	50.18	50.29	50.37
5	47.31	47.50	47.62	47.72	47.80
6	46.37	46.53	46.64	46.72	46.79
7	46.42	46.56	46.65	46.72	46.78
8	47.15	47.27	47.34	47.40	47.45
9	48.37	48.47	48.53	48.59	48.63
10	49.98	50.06	50.12	50.16	50.12

the deformations for plates with stiffer structures. With an increase in the core thickness and Kirchhoff's modulus or with a decrease in the facing thickness, the form of plate deformation has an additional buckling wave.

Table 4. Critical plate loads p_{cr} for different wave numbers m



m	$p_{cr} \text{ [MPa]}$				
	N				
	11	14	17	21	26
0	74.70	75.61	76.05	76.39	76.57
1	86.78	87.72	88.16	88.48	88.69
2	121.70	123.47	124.27	124.87	125.27
3	159.50	165.46	167.18	168.42	169.26
4	195.78	214.02	217.68	219.94	221.45
5	236.00	263.92	275.70	279.59	282.12

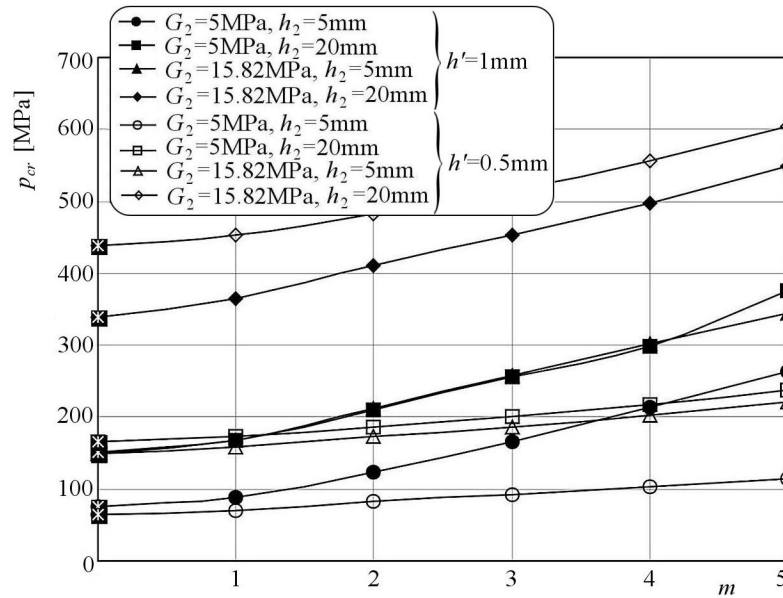


Fig. 4. Critical static load distributions depending on number of buckling waves for plates compressed on inner perimeter

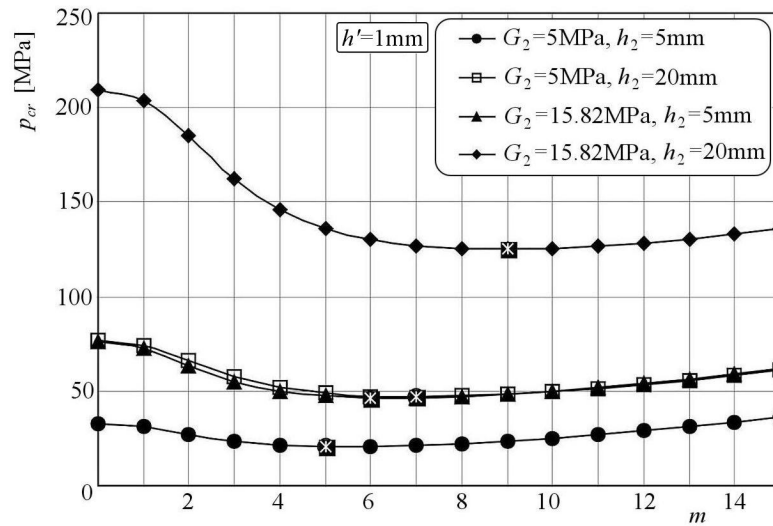


Fig. 5. Critical static load distributions depending on number of buckling waves for plates compressed on outer perimeter with different core thicknesses and material parameters

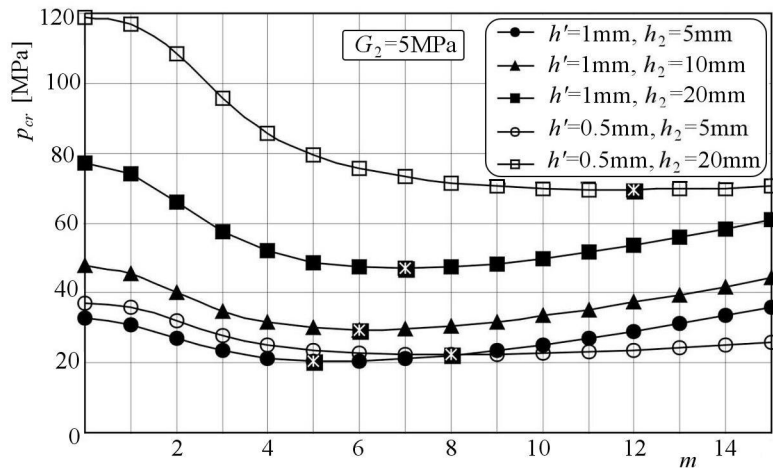


Fig. 6. Critical static load distributions depending on number of buckling waves for plates compressed on outer perimeter with different core and facing thicknesses

5.2. Calculations by finite element method

The presented results of examined plates have been compared with the results obtained using the Finite Element Method (FEM). For this purpose, the computational plate models consistent with the analysed models in the finite

difference method have been built. The fundamental computational model of the plate is a full annulus plate model presented in Fig. 7. Additionally, the plate models in the form of an annular sector as the $1/8$ or $1/6$ part of the annulus have been built – see Fig. 8a,b, respectively.

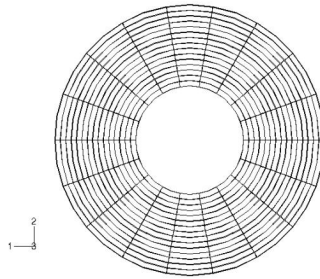


Fig. 7. Full annulus plate model

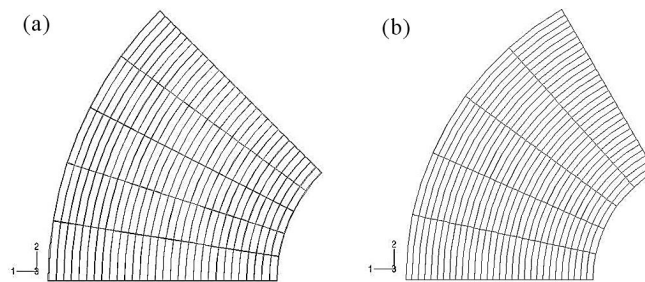


Fig. 8. Annular sector plate model, (a) $1/8$ part of annulus ($\alpha = 45^\circ$), (b) $1/6$ part of annulus ($\alpha = 60^\circ$)

The facing mesh has been built using 3D, 9-node shell elements, but the core mesh was made of 3D, 27-node solid elements. The outer surfaces of facing mesh elements have been connected with the outer surfaces of core elements using the surface contact interaction. The deformations of the inner and outer plate edges have been limited by the support conditions without the possibility of relative displacements of facings in their clamped edges. There is no limitation to the deformation, which was earlier formulated by the condition of equal deflections of each plate layer. The calculations were carried out at the Academic Computer Center CYFRONET-CRACOW (KBN/SGLORIGIN_2000/PŁódzka/030/1999) using the ABAQUS system.

The symmetry conditions enabling the observation of such forms of plate deformations for which the length of a single circumferential wave is included or is a multiple of the angle of an annular sector have been imposed on the side

edges of the annular sector plate models. The computational results of plate models built in the form of annular sectors (Fig. 8) compared with the results of the full annulus plate model (Fig. 7) allow the evaluation of correctness of the FEM-based calculations. The computational capability of the program enabled creation of plate meshes for the annular sector model thicker than those for the full annulus model, hence the accuracy of the results could be greater. The results presented in Fig. 9 and in Tables 5, 6, 7 for plates with the facing thickness $h' = 0.001$ m show some quantitative discrepancy in values of the critical loads.

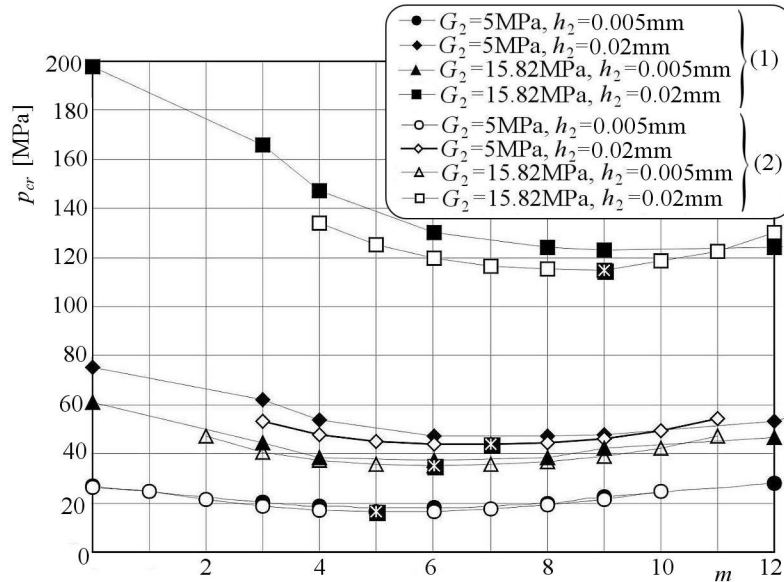


Fig. 9. Distribution of critical static loads of plates modelled as annular sectors or full annulus; (1) annular sector model, (2) full annulus

The presented in Tables 5, 6, 7 critical loads p_{cr} and forms of buckling are given in the increasing order up from the minimal value to numbers obtained for the full annulus plate model. All results concern the plate models loaded at the outer edge of facings. The presented results are comparable, however some differences in the range of higher values of critical loads depending on the kind of computational plate model are observed. One can notice some sensitivity of numerical results with depend on the computational model using FEM. Some detailed remarks concerning calculations of plates loaded at inner facing edges, which are differently modelled were presented by Pawlus (2002, 2004, 2005). The numerical calculation of the full annulus plate model loaded at the inner edges confirms the observation that the minimal critical loads corresponds

Table 5. Critical stresses calculated by means of FEM for plate models with parameters: $h_2 = 0.005$ m, $G_2 = 5$ MPa

m	p_{cr} [MPa]		
	Full annulus plate model	Annular sector of plate model	
		$\alpha = 45^\circ$	$\alpha = 60^\circ$
5	16.48	–	–
6	16.75	–	17.92
4	17.02	18.76	–
7	17.68	–	–
3	18.65	–	20.22
8	19.25	19.74	–
9	21.49	–	22.48
2	21.52	–	–
10	24.71	–	–
1	24.87	–	–
0	26.44	27.06	29.98

Table 6. Critical stresses calculated by means of FEM for plate models with parameters: $h_2 = 0.005$ m, $G_2 = 15.82$ MPa

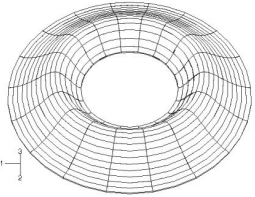
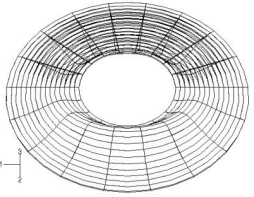
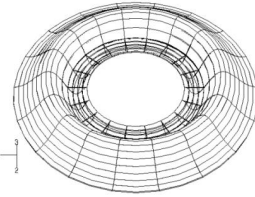
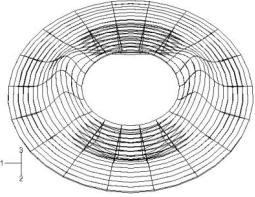
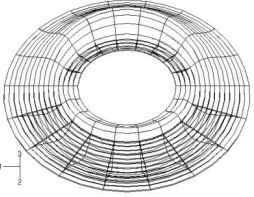
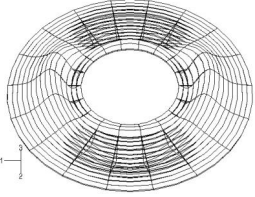
m	p_{cr} [MPa]		
	Full annulus plate model	Annular sector of plate model	
		$\alpha = 45^\circ$	$\alpha = 60^\circ$
6	35.04	–	36.74
5	35.46	–	–
7	35.57	–	–
8	36.94	38.35	–
4	37.19	38.37	–
9	38.98	–	39.86
3	40.87	–	44.24
10	42.48	–	–
2	47.01	–	–

to the regular axi-symmetrical form ($m = 0$) of plate buckling. Exemplary critical loads in the increasing order for a plate with layer thicknesses equal: $h' = 0.001$ m, $h_2 = 0.005$ m and with core Kirchhoff's modulus $G_2 = 5$ MPa are presented in Table 8.

Table 7. Critical stresses calculated by means of FEM for plate models with parameters: $h_2 = 0.02$ m, $G_2 = 15.82$ MPa

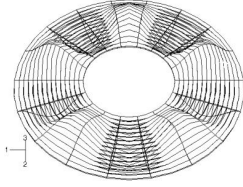
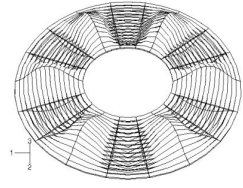
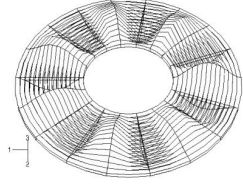
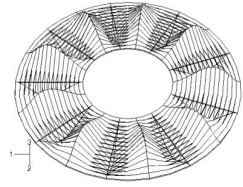
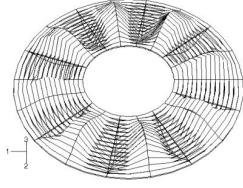
m	p_{cr} [MPa]		
	Full annulus plate model	Annular sector of plate model	
		$\alpha = 45^\circ$	$\alpha = 60^\circ$
9	115.10	–	123.23
8	115.26	124.43	–
7	116.52	–	–
10	118.41	–	–
6	119.53	–	130.13
11	122.55	–	–
5	125.01	–	–
12	129.98	–	124.03
4	134.29	147.01	–

Table 8. Critical stresses and forms of buckling of plates loaded at inner perimeter of facings ($d_1 = 1$, $d_2 = 0$)

p_{cr} [MPa]		
64.08	75.75	107.04
$m = 0$	$m = 1$	$m = 0, n = 1$
		
109.89	113.95	141.35
$m = 2$	$m = 1, n = 1$	$m = 2, n = 1$
		

n – number of waves in radial direction

Table 9. Critical stresses and forms of buckling of plates loaded at outer perimeter of facings ($d_1 = 0$, $d_2 = 1$)

Parameters of plate $h' / h_2 / G_2$ [m] / [m] / [MPa]	p_{cr} [MPa]			Form of buckling
	FDM	FEM		
		Full annulus plate model	Annular sector of plate model	
0.001 / 0.005 / 5.0	20.52	16.48	–	$m = 5$ 
0.001 / 0.01 / 5.0	29.42	25.85	27.93	$m = 6$ 
0.001 / 0.02 / 5.0	46.95	43.71	–	$m = 7$ 
0.001 / 0.005 / 15.82	46.53	35.04	36.74	$m = 6$
0.001 / 0.02 / 15.82	125.11	115.1	123.23	$m = 9$ 
0.0005 / 0.005 / 5.0	22.37	–	–	$m = 8$ 
	–	19.6	–	$m = 7$

6. Conclusions

Comparing the results obtained using the two presented methods: Finite Difference Method (FDM) and Finite Element Method (FEM), quantitative correctness and qualitative consistency have been observed. Suitable results of critical static loads of plates calculated in the FDM and FEM with their forms of buckling are presented in Table 9. The critical loads of the annular sector plate model built in FEM show better consistency with the results of plates calculated in the FDM. For plates with thin facings ($h' = 0.0005$ m), a difference in the buckling form calculated in the FDM and in FEM is observed. The number of waves is equal to $m = 8$ and $m = 7$, respectively.

Analysing the results of critical static loads with forms of buckling of annular sandwich double-clamped plates determined by the two presented methods, it can be concluded:

- in the case of loading of the inner plate perimeter, the minimal value of compressive static critical load is found for a regular axi-symmetrical form of loss of the plate static stability
- in the case of loading of the outer plate perimeter, the minimal critical static loads and the numbers of buckling waves depend on the geometrical and material parameters: with the increase in the plate stiffness, the critical loads and numbers of circumferential buckling waves increase, too.

References

1. ABAQUS/Standard. User's Manual, version 6.1, 2000, Hibbitt, Karlsson and Sorensen, Inc.
2. CHEN Y.R., CHEN L.W., WANG C.C., 2006, Axisymmetric dynamic instability of rotating polar orthotropic sandwich annular plates with a constrained damping layer, *Composite Structures*, **73**, 2, 290-302
3. DUMIR P.C., SHINGAL L., 1985, Axisymmetric postbuckling of orthotropic thick annular plates, *Acta Mechanica*, **56**, 229-242
4. DUMIR P.C., JOSHI S., DUBE G.P., 2001, Geometrically nonlinear axisymmetric analysis of thick laminated annular plate using FSDT, *Composites: Part B*, **32**, 1-10

5. KRIZHEVSKY G., STAVSKY Y., 1996, Refined theory for vibrations and buckling of laminated isotropic annular plates, *International Journal of Mechanical Sciences*, **38**, 5, 539-555
6. MAJEWSKI S., MAĆKOWSKI R., 1975, Pelzanie spienionych tworzyw sztucznych stosowanych jako rdzeń płyt warstwowych, *Inżynieria i Budownictwo*, **3**, 127-131
7. PAWLUS D., 1996, Zachowanie pierścieniowych płyt lepkosprężystych przy obciążeniach zmiennych, Ph.D. Thesis, Politechnika Łódzka Filia w Bielsku-Białej
8. PAWLUS D., 2002, Obliczenia statycznych obciążeń krytycznych trójwarstwowych, osiowosymetrycznych płyt pierścieniowych, *Czasopismo Techniczne*, **6-M**, Wydawnictwo Politechniki Krakowskiej, 71-86
9. PAWLUS D., 2003, Calculations of three-layered annular plates under lateral loads, *Studia Geotechnica et Mechanica*, **XXV**, 3/4, 89-109
10. PAWLUS D., 2004, Obliczenia metodą elementów skończonych trójwarstwowych płyt pierścieniowych poddanych obciążeniom w ich płaszczyźnie, *III Sympozjum Kompozyty. Konstrukcje warstwowe*, Wrocław-Karpacz, 119-128
11. PAWLUS D., 2005, Dynamic stability problem of three-layered annular plate under lateral time-dependent load, *Journal of Theoretical and Applied Mechanics*, **43**, 2, 385-403
12. TROMBSKI M., WOJCIECH S., 1981, Płyta pierścieniowa o ortotropii cylindrycznej obciążona w swej płaszczyźnie ciśnieniem zmiennym w czasie, *The Archive of Mechanical Engineering*, **XXVIII**, 2
13. ROMANÓW F., 1995, *Wytrzymałość konstrukcji warstwowych*, WSI w Zielonej Górze
14. VOLMIR C., 1967, *Stability of Deformed System*, Science, Moskwa (in Russian)
15. WANG H.J., CHEN L.W., 2003, Axisymmetric dynamic stability of sandwich circular plates, *Composite Structures*, **59**, 99-107
16. WOJCIECH S., 1978, Stateczność dynamiczna ortotropowej płyty pierścieniowej obciążonej w swojej płaszczyźnie ciśnieniem zmiennym w czasie, Ph.D. Thesis, Politechnika Łódzka
17. WOJCIECH S., 1979, Numeryczne rozwiązanie zagadnienia stateczności dynamicznej płyt pierścieniowych, *Journal of Theoretical and Applied Mechanics*, **17**, 2

Rozwiązanie zagadnienia stateczności statycznej pierścieniowych płyt trójwarstwowych z rdzeniem miękkim

Streszczenie

W pracy przedstawiono rozwiązania stateczności statycznej trójwarstwowych płyt pierścieniowych o symetrycznej strukturze poprzecznej z piankowym rdzeniem miękkim. Zasadniczą częścią rozwiązania jest wyprowadzenie układu równań różniczkowych opisujących ugięcia płyty oraz wykorzystanie metody różnic skończonych i wyznaczenie krytycznych obciążeń płyt poprzez rozwiązanie zagadnienia wartości własnych. Wyznaczonym wartościom ciśnień krytycznych płyt obciążonych na wybranym brzegu ich okładzin odpowiadają postacie deformacji płyt, które określa liczba m fal poprzecznych na obwodzie płyty. Otrzymane wyniki pod względem ilościowym i jakościowym porównano z wynikami obliczeń metodą elementów skończonych przedstawionych modeli płyt. Sformułowano uwagi końcowe dotyczące form utraty stateczności statycznej analizowanych płyt o strukturze warstwowej. Artykuł stanowi uzupełnienie pracy Pawlus (2005) dotyczącej obliczeń stateczności dynamicznej płyt i rozwinięcie na przypadki sfalowanych form deformacji rozwiązania problemu stateczności statycznej płyt rozpatrywanego wcześniej, min. w pracy Pawlus (2002) w zakresie tylko obrotowych, osiowo-symetrycznych form utraty ich stateczności.

Manuscript received February 16, 2006; accepted for print March 20, 2006